J. Fluid Mech. (1992), *vol.* 239, *pp.* 511–522
Printed in Great Britain

Stability of salt fingers with negligible diffusivity

By L. N. HOWARD[1] AND G. VERONIS[2]

[1] Mathematics Department, Florida State University, Tallahassee, FL 32306, USA

[2] Geology and Geophysics Department, Yale University, New Haven, CT 06511, USA

(Received 13 September 1991 and in revised form 1 December 1991)

An array of long, vertically uniform salt fingers in an environment with salt input from above, fresh input from below, a vertically constant, stabilizing temperature gradient and negligible salt diffusion is found to be unstable to perturbations with vertical structure. The maximum growth rate and the form of the instability are derived for fingers with widths that yield maximum buoyancy flux in the unperturbed state. The dependence of the instability on the magnitude of the imposed salt difference is obtained for the heat–salt system. A direct (non-oscillatory) mode with a vertical scale of the order of the buoyancy-layer thickness is the most unstable when the amplitude of the vertical velocity of the fingers is large. The instability is due to the shear flow between rising and sinking fluid in adjacent fingers and is relatively unaffected by the perturbation buoyancy. When the driving is weaker, the dominant instability involves the same processes as for the basic fingers, i.e. perturbation buoyancy, viscosity and diffusion, and the mode becomes oscillatory in time. All of the most unstable modes derived here have a vertical scale of the order of the buoyancy-layer thickness. Both the direct and the oscillatory modes have net horizontal flows that vary with the vertical coordinate and time and in finite amplitude could cause the fingers to incline toward the horizontal. The oscillatory mode involves pairs of fingers so the emerging behaviour could include a kind of period doubling.

1. Introduction

Salt fingers are generated when warm, salty water lies above cool, fresh water and the relationship, $R_\rho \tau < 1$, is satisfied (Stern 1960). Here, R_ρ is the density ratio of the stabilizing temperature gradient ($\alpha \bar{T}_z$) or difference ($\alpha \Delta T$) to the destabilizing salt gradient ($\beta \bar{S}_z$) or difference ($\beta \Delta S$) and $\tau (< 1)$ is the ratio of salt diffusivity to that of temperature.

These long, slender features can arise from a variety of initial configurations. A commonly assumed initial state is one with a layer of uniformly warm, salty water above a layer of cold, fresh water, the two separated by an interface. Laboratory experiments, e.g. in a Hele–Shaw cell (Taylor & Veronis 1986), may start with a physical barrier between the layers. In nature and in some laboratory studies a lateral intrusion of warm, salty water into a cold, fresh environment will give rise to salt fingers at the base of the warm, salty layer. Initially, very thin fingers are generated almost instantaneously and create a salt-finger zone of approximately 1–2 cm in height, in which the stabilizing mean temperature gradient is essentially uniform in the vertical. As the height of the zone increases, the mean vertical temperature gradient decreases and the optimal width of the fingers increases ($\sim (\partial T/\partial z)^{-\frac{1}{4}}$, see below). In the Taylor & Veronis (1986) experiments new fingers were continually formed at the outer edges of the finger zone where the temperature

gradient is small (so that the finger width is larger). These fingers penetrated into the finger zone, displacing narrower fingers.

The evolution of such a system depends strongly on the size of the destabilizing density anomaly associated with the salinity difference, ΔS. If ΔS is large, the fluid will flow rapidly through the finger and will deposit the relatively large salt anomaly at the edge of the finger zone, so that a destabilizing density layer is formed giving rise to active, convective layers in the reservoirs above and below. In such a case the fluid may move through the fingers so rapidly that no instability has time to grow significantly and the system will evolve with time, unaffected by any instabilities. Here, a salt-finger zone sandwiched between two convecting layers would be a stable, evolving system until the fingers become long and potentially unstable.

When ΔS is smaller or the finger length is large enough, the fluid will take more time to traverse the finger zone and instabilities may have time to alter the fingers. Salt diffusion, which tends to redistribute the salt anomaly laterally, will thereby decrease the buoyancy anomaly (and therefore, the vertical velocity) in the fingers and allow the instability time to manifest itself. The evolution of the system in this case is more complicated because it will depend on how the finite-amplitude salt fingers alter the mean background gradients.

A second initial configuration is one with a layer of smooth temperature and salinity gradients sandwiched between the reservoirs. The layer may be deliberately produced or it may emerge from the mixing that occurs when one tries to generate two layers by pouring the (lighter) warm, salty water onto the top of the cold, fresh layer. In almost all of these situations the mixing does not create vertically smooth gradients but rather a layer with homogeneous patches of fluid each of which has different T, S properties. When such a patchy layer was generated in the Taylor & Veronis (1986) experiments, salt fingers appeared in isolated areas (presumably, at the base of the warm, salty patches). Gradually, the fingers merged with other fingers above and below until after a considerable time the entire mixed layer was filled with a very regular pattern of salt fingers.

Another set-up, a combination of the two mentioned above, is to start with a two-layer system and to continue to maintain fixed concentrations in the two reservoirs. The thickness of the salt-finger zone will adjust by itself to an appropriate value and remain constant.

Models of salt fingers assume one of the configurations mentioned above. When the background consists of a relatively stable temperature gradient and a mildly destabilizing salt gradient (τR_ρ near 1), the fingers are vertically long, the fluid velocities are small and the system evolves slowly. Therefore, there must be significant horizontal diffusion of salt between up- and down-going fingers. Stern (1975) analysed a pattern of fingers using this idea.

When the initial state is two-layered and the destabilizing salt difference, ΔS, is much greater than that required for marginal instability ($R_\rho \tau^{\frac{3}{2}} < 1$, Huppert & Manins 1973), fingers evolve very rapidly and the destabilizing property is very nearly uniform in a finger. In this case it is more appropriate to analyse the system assuming that the horizontal distribution of salt is $\frac{1}{2}\Delta S$ in sinking fingers and $-\frac{1}{2}\Delta S$ in rising ones.

Howard & Veronis (1987, hereafter referred to as HV) calculated the horizontal distributions of vertical velocity, w, and temperature, T, based on such a salinity distribution and a constant mean temperature gradient, $\bar{T}_z$. Their zero-order model assumed the fingers to be very long compared to the width, and the diffusion of salt to be negligible. The analysis showed that the finger width must be small enough to

allow the stabilizing temperature to diffuse horizontally between up- and down-going fingers so that the destabilizing salinity can drive salty (fresh) fluid downward (upward). The horizontal scale, L, of the fingers is given by $(4\kappa_T \nu/g\alpha\bar{T}_z)^{\frac{1}{4}}$, where κ_T is the thermometric diffusivity, ν is the kinematic viscosity and g is the acceleration due to gravity.

This scale was first derived by Prandtl (1952), who showed that in a stably stratified fluid a sidewall boundary layer allows a smooth transition between the temperature of the inviscid interior and the value imposed at the wall. Horizontal diffusion of temperature and vertical velocity balances the vertical advection of mean temperature and the gravitational term respectively in this 'buoyancy layer'. Stern (1960) showed that the same horizontal scale determines the width of salt fingers with maximum growth rate in a fluid with imposed temperature and salinity gradients. In all of these situations horizontal diffusion serves to diminish the stabilizing effect of the mean temperature gradient.

Stern's (1969) original study of the stability of salt fingers employed the same assumptions that HV made but he chose a horizontally sinusoidal distribution of salt. When he summarized the salt-finger problem in his book (Stern 1975), he used a vertical salt gradient instead of a salt difference and incorporated horizontal salt diffusion into the analysis. Because the *solutions* for the two models have the same form, it is commonly assumed that the *models* are identical. Yet what Stern (1969) calls an equilibrium model is really an approximate version of the HV model.

The steady solutions for w and T obtained by HV are proportional to the parameter, $Q = \beta\Delta S/L\alpha\bar{T}_z$, where L is the buoyancy-layer thickness. If the temperature gradient is rewritten as $\bar{T}_z = \Delta T/H$, where H is the height of the salt-finger zone, Q becomes $(H/L)(\beta\Delta S/\alpha\Delta T) = (H/L)(1/R_\rho)$, where $R_\rho \geqslant 1$ for salt fingers. Thus, Q contains information about both the density ratio and the aspect ratio, H/L, of the fingers. Recall that in a system evolving from an initial two-layer state the vertical temperature gradient will gradually diminish as the fingers lengthen and the finger width will accordingly increase. Therefore, if the HV model is taken to be an acceptable approximation to such an evolving system at any given time, the parameter Q will grow (parametrically with time) like $H^{\frac{3}{4}}$ (since $L \sim H^{\frac{1}{4}}$).

In this paper we investigate the stability of these quasi-steady salt fingers. A stability analysis will help to determine the conditions under which salt fingers can continue to exist as entities. However, there are certain stages in the evolution of fingers in which stability is not the issue. That must be true during the initial phase of a two-layer configuration when fingers grow rapidly and keep changing. Even so, it will help to know under what conditions an instability can occur and the form that it will take.

The parameter Q appears in the stability analysis also. Since the fingers are assumed to be long, the ratio H/L is always large so Q is large if R_ρ is near unity. Values of Q near unity are possible only for a very stably stratified fluid ($R_\rho \approx H/L$). In such a case, the vertical velocity in the background fingers will be slow and the effect of salt diffusion may become significant so that the zero-order HV model would have to be modified. However, very few laboratory experiments have been carried out with large R_ρ. Furthermore, the range of R_ρ of oceanographic interest is from 1 to 3 and areas with evidence of significant salt-fingering activity have $R_\rho \approx 1.6$. Hence, for long fingers the interesting range is that of large Q. If the fingers are short ($H/L \approx 1$), a basic assumption of the HV model is violated and the variation in z should be taken into account. Probably the only realistic hope is to tackle that system numerically.

The next section includes a brief derivation of the HV zero-order model and the formulation of the stability problem. Section 3 reports the results of the stability analysis. A discussion of the implications of the analysis concludes the paper.

2. Mathematical formulation

The conservation equations for vorticity, heat and salt in two dimensions for a Boussinesq fluid are

$$(\partial_t - \nu\nabla^2)\nabla^2\Psi + g\alpha T_x - g\beta S_x = -\boldsymbol{v}\cdot\boldsymbol{\nabla}\nabla^2\Psi, \tag{2.1a}$$

$$(\partial_t - \kappa_T\nabla^2)T - \bar{T}_z\Psi_x = -\boldsymbol{v}\cdot\boldsymbol{\nabla}T, \tag{2.1b}$$

$$(\partial_t - \kappa_S\nabla^2)S = -\boldsymbol{v}\cdot\boldsymbol{\nabla}S, \tag{2.1c}$$

where ν denotes kinematic viscosity, κ_T thermometric diffusivity, κ_S salt diffusivity, $\rho\alpha = -\partial\rho/\partial T$, $\rho\beta = \partial\rho/\partial S$, $\bar{T}_z$ denotes the mean temperature gradient, and $\boldsymbol{v} = (u, w) = (\Psi_z, -\Psi_x)$.

In (2.1) the temperature has been divided into a value, $\bar{T}$, varying linearly in z, and the remaining part, T. The salinity is the departure from the (constant) mean value in the finger zone. The definition for the stream function is in the definition of $\boldsymbol{v}$.

The variables are non-dimensionalized with

$$\boldsymbol{\nabla} = \frac{\boldsymbol{\nabla}'}{L}, \quad t = \frac{L^2 t'}{\kappa_T}, \quad \boldsymbol{v} = \frac{\kappa_T \boldsymbol{v}'}{L}, \quad T = \tfrac{1}{2}\bar{T}_z L T', \quad S = \tfrac{1}{2}S'\Delta S, \quad L = (4\nu\kappa_T/g\alpha\bar{T}_z)^{\frac{1}{4}},$$

where L is the buoyancy-layer thickness. The dimensionless equations (without the primes) become

$$(\partial_t - \sigma\nabla^2)\nabla^2\Psi + 2\sigma T_x - 2\sigma Q S_x = -\boldsymbol{v}\cdot\boldsymbol{\nabla}\nabla^2\Psi, \tag{2.2a}$$

$$(\partial_t - \nabla^2)T - 2\Psi_x = -\boldsymbol{v}\cdot\boldsymbol{\nabla}T, \tag{2.2b}$$

$$(\partial_t - \tau\nabla^2)S = -\boldsymbol{v}\cdot\boldsymbol{\nabla}S, \tag{2.2c}$$

where $\tau = \kappa_S/\kappa_T$, $\sigma = \nu/\kappa_T$, $Q = \beta\Delta S/\alpha L\bar{T}_z$. Because of the choice of L, the Rayleigh number, $R = g\alpha\bar{T}_z L^4/\nu\kappa_T$, does not appear explicitly. However, the ratio of the salt to the thermal Rayleigh numbers appears in Q. As mentioned in the introduction, when $\bar{T}_z$ is replaced by $\Delta T/H$, the aspect ratio, H/L, also appears explicitly in Q.

2.1. *The small-τ approximation*

The salt-finger model in HV assumes $\tau = 0$ at zero order and a salt difference, ΔS, across the finger zone. The salinity is taken to be $\frac{1}{2}\Delta S$ in descending fingers and $-\frac{1}{2}\Delta S$ in ascending ones. With $\partial/\partial z = 0$ so that $u = 0$, the above equations become

$$\frac{1}{\sigma}w_t - w_{xx} - 2T = 2Q, \tag{2.3a}$$

$$T_t - T_{xx} + 2w = 0, \tag{2.3b}$$

where $Q = \beta\Delta S/\alpha L\bar{T}_z$ in the region $0 \leqslant x \leqslant \pi b$ (πbL is the dimensional finger width). Q changes sign in $-\pi b \leqslant x \leqslant 0$ and the system has periodicity $2\pi b$.

All solutions to these equations approach the following steady state (subscript s) in $0 \leqslant x \leqslant \pi b$ (which is thus stable with respect to perturbations independent of z):

$$w_s = -Q\left\{\frac{\sinh x \sin(\pi b - x) + \sin x \sinh(\pi b - x)}{\cosh \pi b + \cos \pi b}\right\}, \tag{2.4a}$$

$$T_s = -Q\left\{\frac{\cosh x \cos(\pi b - x) + \cos x \cosh(\pi b - x)}{\cosh \pi b + \cos \pi b} - 1\right\}. \tag{2.4b}$$

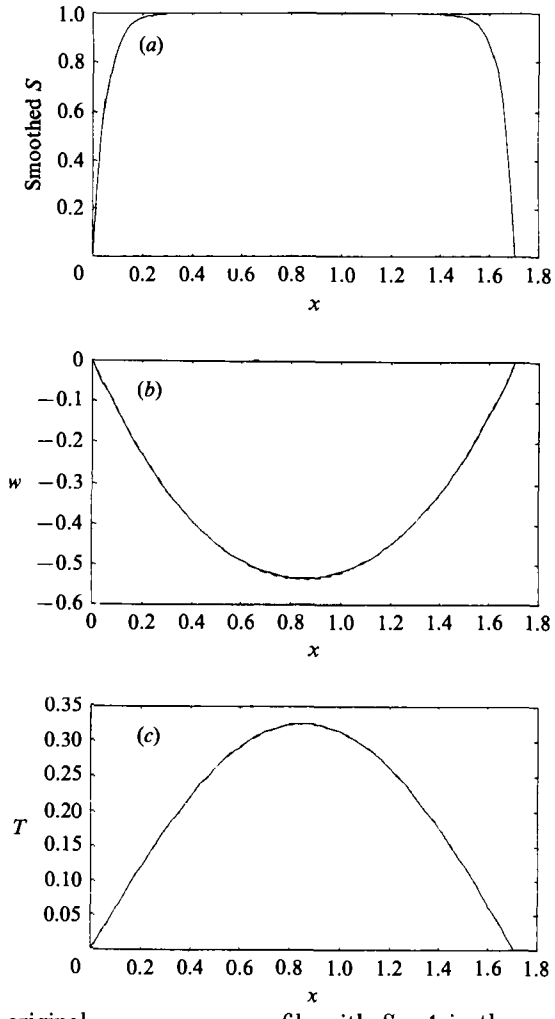

FIGURE 1. (*a*) The original, square-wave profile with $S = 1$ in the range $0 \leqslant x \leqslant \pi b = 1.7$. Also shown is the smoothed salinity profile obtained with $\gamma = 20$ (in (2.8)) for a finger in the region $0 \leqslant x \leqslant \pi b$. (*b*) The vertical velocity generated by the square S superimposed on the vertical velocity due to the smoothed S in (*a*). The two w are essentially coincident. (*c*) As in (*b*) but for temperature.

In the range $-\pi b \leqslant x \leqslant 0$, Q is replaced by $-Q$ (w and T change sign) and $\pi b - x$ is replaced by $\pi b + x$. In HV it was shown that the buoyancy flux achieves its maximum value of 0.251 for $b = 0.542$. The solutions w_s and T_s for this case are shown in figure 1(*b*) and 1(*c*) respectively.

Although a correction for S due to small salt diffusion is given in HV, we shall here restrict our attention to the stability of the configuration described by the zero-order solution (2.4).

2.2. *Stability problem*

When perturbations $T(x, z, t)$, $S(x, z, t)$, $\Psi(x, z, t)$ are added to the steady solution the linear equations for T, S, and Ψ take the form

$$\nabla^2 \Psi_t = \sigma \nabla^4 \Psi - 2\sigma T_x + 2\sigma Q S_x + w_{sxx} \Psi_z - w_s \nabla^2 \Psi_z, \tag{2.5a}$$

$$T_t = \nabla^2 T + 2\Psi_x - T_{sx} \Psi_z - w_s T_z, \tag{2.5b}$$

$$S_t = -S_{sx} \Psi_z - w_s S_z. \tag{2.5c}$$

Since the coefficients are spatially periodic functions, this system can be solved using Floquet theory by substituting

$$(\Psi, T, S) = \sum_{n=-N}^{N} (\Psi_n, \mathrm{i}T_n, \mathrm{i}S_n) \exp\{\lambda t + \mathrm{i}[mz + (k+n)x]/b\} \tag{2.6}$$

in the region $-\pi b \leqslant x \leqslant \pi b$, where $\mathrm{i}k/b$ is the (Floquet) characteristic exponent. (It is convenient to write the Fourier coefficients for T and S as $\mathrm{i}T_n$ and $\mathrm{i}S_n$.) The equations that the component coefficients must satisfy are

$$\lambda \Psi_j = -\sigma K_j \Psi_j - \frac{2(k+j)\sigma}{bK_j}(T_j - QS_j) - \frac{mQ}{\pi K_j}\sum{}' \left\{ \frac{\frac{2n_1}{b} - K_n}{n_1^2 + b^2} + \frac{\frac{2n_2}{b} + K_n}{n_2^2 + b^2} \right\} \Psi_n, \tag{2.7a}$$

$$\lambda T_j = -K_j T_j + \frac{2(k+j)}{b}\Psi_j + \frac{mQ}{\pi b}\sum{}' \times \left\{ \left[\frac{2b-n-j}{n_1^2+b^2} + \frac{2b+n-j}{n_2^2+b^2} \right] \Psi_n + \left[\frac{b}{n_1^2+b^2} - \frac{b}{n_2^2+b^2} \right] T_n \right\}, \tag{2.7b}$$

$$\lambda S_j = \frac{m}{\pi}\sum{}' \left\{ \frac{2\Psi_n}{b^2} + Q\left[\frac{1}{n_1^2+b^2} - \frac{1}{n_2^2+b^2} \right] S_n \right\}, \tag{2.7c}$$

where $K_j = [(k+j)^2 + m^2]/b^2$, $n_1 = n-j-b$, $n_2 = n-j+b$, and the summation $\sum'$ extends over odd values of $n-j$. The infinite system is invariant under the transformation $k \to -k$ and $k \to 1+k$. However, for finite N, when k is replaced by either $1+k$ or $-k$, the series loses its symmetry and the value of λ is altered. Furthermore, an even value of N leads to a solution for λ that differs from that obtained with odd N. These discrepancies are particularly highlighted in this problem because S_s has a finite discontinuity at the boundaries $x = n\pi b$, $n = 0, \pm 1, \pm 2, \ldots$, where the Fourier representation for S_s exhibits a Gibbs phenomenon and $\partial S_s/\partial x$ is a Dirac delta function with constant Fourier coefficients.

We get around this difficulty by smoothing the discontinuity of the steady salinity using the convenient form

$$S_s = -\frac{1 + \mathrm{e}^{-\gamma\pi b} - \mathrm{e}^{-\gamma x} - \mathrm{e}^{-\gamma(\pi b - x)}}{1 + \mathrm{e}^{-\gamma\pi b} - 2(1 - \mathrm{e}^{-\gamma\pi b})/\gamma\pi b} = -\frac{\cosh(\frac{1}{2}\gamma\pi b) - \cosh\gamma(x - \frac{1}{2}\pi b)}{\cosh(\frac{1}{2}\gamma\pi b) - 2\sinh(\frac{1}{2}\gamma\pi b)/\gamma\pi b}, \quad 0 < x < \pi b, \tag{2.8a}$$

$$S_s = \frac{1 + \mathrm{e}^{-\gamma\pi b} - \mathrm{e}^{\gamma x} - \mathrm{e}^{-\gamma(\pi b + x)}}{1 + \mathrm{e}^{-\gamma\pi b} - 2(1 - \mathrm{e}^{-\gamma\pi b})/\gamma\pi b} = \frac{\cosh(\frac{1}{2}\gamma\pi b) - \cosh\gamma(x + \frac{1}{2}\pi b)}{\cosh(\frac{1}{2}\gamma\pi b) - 2\sinh(\frac{1}{2}\gamma\pi b)/\gamma\pi b}, \quad -\pi b < x < 0. \tag{2.8b}$$

(Essentially, the smoothed S_s incorporates an effect similar to that of small salt diffusion. For the case with $\tau = 0$, S_s in the basic problem appears only as a forcing function in the vorticity equation. Any form which is a function of x alone satisfies the convective salinity equation since $u = 0$.)

As $\gamma \to \infty$ this expression approaches -1 in $0 < x < \pi b$ and $+1$ in $-\pi b < x < 0$. A finite value of γ smooths out the discontinuities in S_s as shown in figure 1 (*a*) for $\gamma = 20$. However, the vertical velocity and temperature fields are practically unaffected by the value of γ (for $\gamma \geqslant 15$) as can be seen in figures 1 (*b*) and 1 (*c*). (Because w_s and T_s vanish where S_s changes sign, the effect of the discontinuity in the salinity is very small near those points.) Therefore, for the stability problem the forms in (2.4) have been used for w_s and T_s, even though the salinity has been

smoothed with $\gamma = 20$. Eliminating the discontinuity in S_s also eliminates the large amplitude at wavenumber N so that expansions with even and odd N tend toward the same value of λ as N becomes large.

3. Results of the stability calculations

For all calculations the value of the Prandtl number, σ, was 7 (corresponding to salt water), and the parameter, b, was 0.542, the value that yields maximum buoyancy flux for the basic finger solution. For each value of Q calculations were made for $0 \leqslant m \leqslant 3$ and $0 \leqslant k \leqslant 1$ in increments of 0.05 to determine the specific values of m and k that lead to maximum growth rate. In the neighbourhood of the maximum value of λ increments of 0.01 were used. The values of λ varied smoothly with k, m and Q.

The number of horizontal wavenumbers required for a convergent solution depends on the value of Q. For $Q \geqslant 10$ a value of $N = 40$ suffices to give $\mathrm{Re}\,(\lambda)$ correct to at least three significant digits. That means that $\mathrm{Re}\,(\lambda)$ changes by less than $10^{-3}\mathrm{Re}\,(\lambda)$ when k is replaced by $1+k$ or by $-k$ or when N is increased to 50. (Recall that for $N = \infty$ the system is invariant to $k \to 1+k$ or $k \to -k$.) With $Q = 1$ it is necessary to use $N = 140$ to obtain values of $\mathrm{Re}\,(\lambda)$ that change by as little as 1% when $k \to 1+k$ or $k \to -k$ or $130 \leqslant N \leqslant 139$.

$Q = 0.1$ requires an even larger value of N. Results are reported below only for $Q \geqslant 1$. Since the basic fingers are required to be long and narrow for the validity of the present analysis, values of Q below 1 are achieved only when the stability parameter, R_ρ, is large ($> H/L$). That would take the system out of the range of physical interest (and even out of the range of possibility, since R_ρ cannot exceed τ^{-1} for long fingers).

Table 1 contains a summary of the values of the important parameters, N, K, M, and λ, for several values of Q. In all cases with $Q \geqslant \sigma$ maximum growth occurs with λ real and with zero for the characteristic exponent, k. Asymptotically, $\lambda \to 0.3Q$ and $m \to 0.68$, so the total vertical wavenumber (m/b) settles to 1.25. Thus, a full vertical wavelength of the unstable mode is about 1.5 times the wavelength of a pair of fingers (one up and one down). Since the buoyancy-layer scale was used to non-dimensionalize the spatial coordinates, this means that the vertical scale of the preferred mode is of the order of the buoyancy-layer thickness.

The basic vertical velocity (proportional to Q) is large in this asymptotic limit and the instability is due to the large shear between rising and falling fluid in adjacent fingers. To test the importance of the density for the perturbation velocity the Prandtl number was set to zero for the case $Q = 1000$, thereby removing both T and S from the vorticity equation. The effect on λ was negligible; the growth rate changed by 1% and the alteration in the stream function was undetectable. Essentially this is an unmodified shear-flow instability. (We obtained the same asymptotic results without Floquet theory by numerical integration of the vorticity equation with periodic boundary conditions in x and with no buoyancy term.)

Qualitatively, the system behaves in the same way for values of Q down to $\sigma\,(= 7)$. Figure 2 shows $\Psi_s + 0.5\Psi$ (both Ψ_s and Ψ are normalized) for $Q = 1000$ and 30. The two graphs are nearly the same. (The abscissa is scaled by b/m, so the real vertical distances in the two graphs differ by about 25%.)

The perturbation stream function for these large values of Q has a net horizontal flow at any given value of z, as shown in figure 3(a) for $Q = 30$. The flow pattern given by $\Psi + 5\Psi_s$ is strongly inclined to the horizontal in thin bands as shown in figure 3(b). Of course, as the perturbation grows it must alter the background mean field;

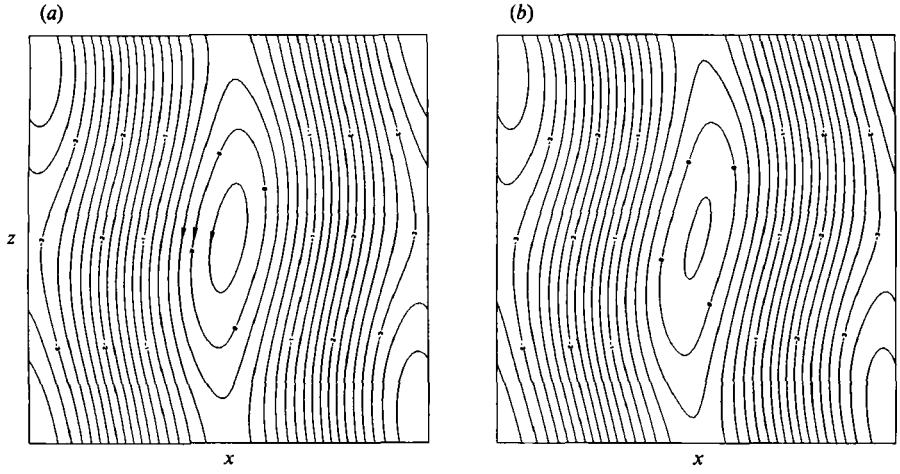

FIGURE 2. (a) Contours of $\Psi_s + 0.5\Psi$ for the most unstable mode ($Q = 1000$, $k = 0$, $m = 0.68$) in a region extending one wavelength in x and one in z. (b) As in (a) but for $Q = 30$, $k = 0$, $m = 0.55$. The (nearly identical) pattern of flow in (a) and (b) represents the most unstable mode for $Q > \sigma$.

Q	N	k	m	λ
1	140	0.5	0.55	$0.0121 \pm 0.363i$
10	40	0	0.40	1.274
10	40	0.5	0.55	$1.063 \pm 3.304i$
30	40	0	0.55	6.308
10^2	40	0	0.65	27.44
10^3	40	0	0.68	301.6
10^4	40	0	0.68	3034.0

TABLE 1. Values of N, k, m and λ for modes with maximum growth rate

therefore, this simple superposition is meant only as an indication of the type of effect that the instability may have. Also, these are instantaneous streamlines (not particle paths) and may not represent the actual flow of the fluid. A full analysis would treat the interaction of mean and perturbation. It is interesting that attempted observations of salt fingers in the CSALT expedition revealed a striated pattern that was more horizontal than vertical (Kunze, Williams & Schmitt 1987). It is at least possible that the instability derived here may lead to more horizontally inclined features in the fully developed system.

A plot of $\rho_s + 2\rho$, with ρ and ρ_s normalized, is depicted for $Q = 30$ in figure 3(c). The perturbation density has its largest amplitude near the sidewalls of the fingers. That appears to be a characteristic feature of the perturbed fingers (see also figure 4b) but, as mentioned earlier, the density plays no role in the instability when Q is large.

When the value of Q is dropped to 10, the mode with the maximum growth rate is still of the same type as described above. However, the next fastest growing mode occurs for $k = 0.5$, $m = 0.55$ and λ is complex with $\mathrm{Re}(\lambda)$ only 20% below the maximum value. (This mode becomes the dominant one for $Q < \sigma$. i.e. when the effects of diffusion become more important than those due to advection.) The flow pattern for $\Psi_s + 0.5\Psi$ at zero phase is shown in figure 4(a) for the region $0 \leqslant x \leqslant 4\pi b$ (two up and two down cells) and for two wavelengths in z. This pattern travels vertically downward (the behaviour is like $\exp[\mathrm{i}(mz/b \pm \lambda_i t)]$ for the mode with $\pm\lambda_i$). The case with $+\lambda_i$ is depicted in figure 4; it has a wavy downward velocity and a

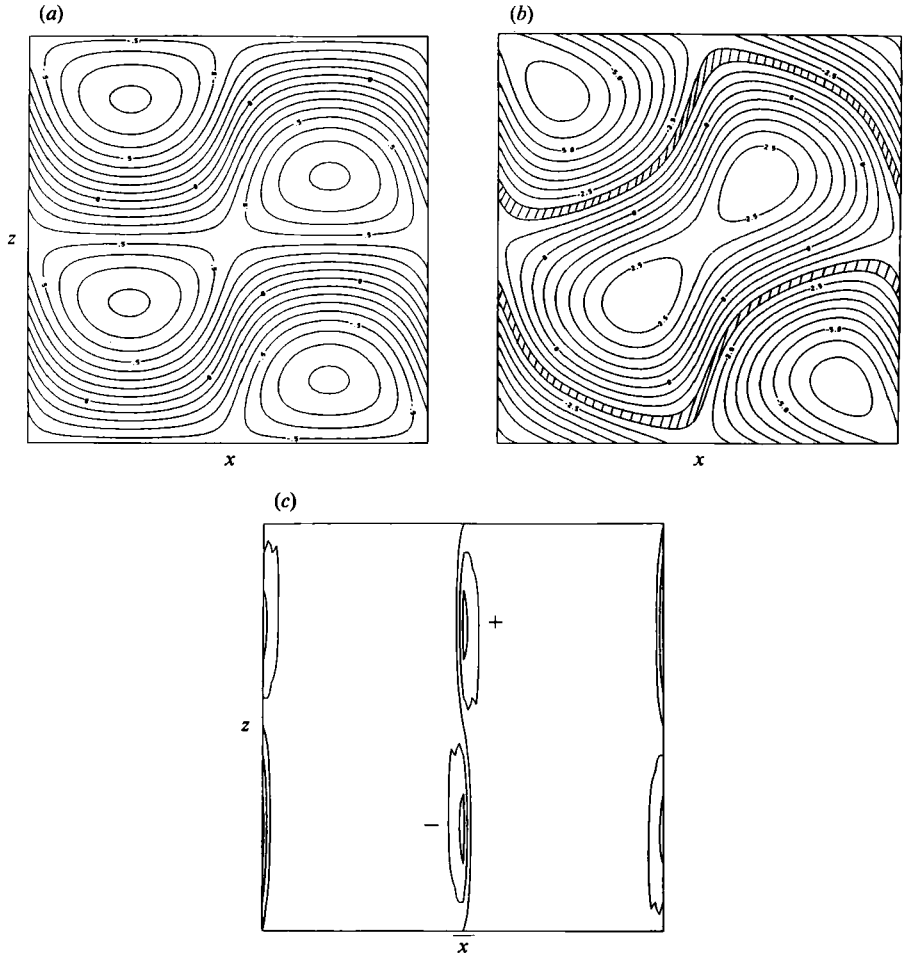

FIGURE 3. (*a*) Contours of the perturbation stream function, Ψ, for $Q = 30$, $k = 0$, $m = 0.55$. The pattern is periodic in x and z. There is a net horizontal flow at each level of z. (*b*) Contours of $\Psi_s + 5\Psi$ for the same case show a band of flow from right to left (hatched upper) and from left to right (hatched lower). (*c*) A few contours of $\rho_s + 2\rho$ for the same case. A positive (negative) density anomaly is indicated by $+(-)$.

more uniform upward flow with closed circulation contours in between. Contours for the density field, $\rho_s + 2\rho$, are shown in figure 4(*b*). Maximum and minimum density values are marked + and −. Vertical flow is inhibited where the density is maximum.

When $Q = 1$ the mode with maximum growth rate has complex λ with $k = 0.5$ and $m = 0.55$. The perturbation stream function for the two modes (with both $+\lambda_i$ and $-\lambda_i$) forms a standing wave pattern which is shown in figure 5(*a*) for $0 \leqslant x \leqslant 4\pi b$ and for two wavelengths in z. The pattern is periodic in x so there is a new flow to the right or left depending on the value of z. This perturbation flow oscillates in time.

A plot of the composite stream function, $\Psi_s + 0.5(\Psi(\lambda) + \Psi(\lambda^*))$, appears in figure 5(*b*). The bands of unidirectional horizontal flow are modified by the mean velocity, w_s. Because the perturbation has a carrier wave with twice the wavelength of the basic velocity, the same structure appears in the composite flow. There is some indication from numerical experiments that there is a period doubling in the pattern of fluid emerging from a salt finger zone, i.e. just above and below the finger zone the

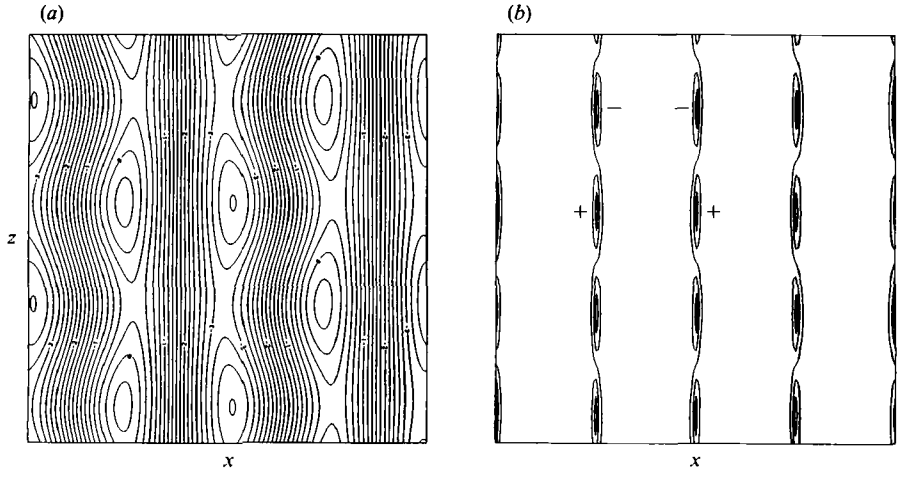

FIGURE 4. (a) Contours of $\Psi_s + 0.5\Psi$ for the travelling wave mode when $Q = 10$, $k = 0.5$, $m = 0.55$. The flow is down along the wavy contours and up along the straighter ones. With $k = 0.5$ a full wavelength in x corresponds to two wavelengths of the steady flow Ψ_s. The vertical range extends two wavelengths in z. (b) Contours of $\rho_s + 2\rho$ for the same case. A positive (negative) density anomaly is indicated by $+(-)$.

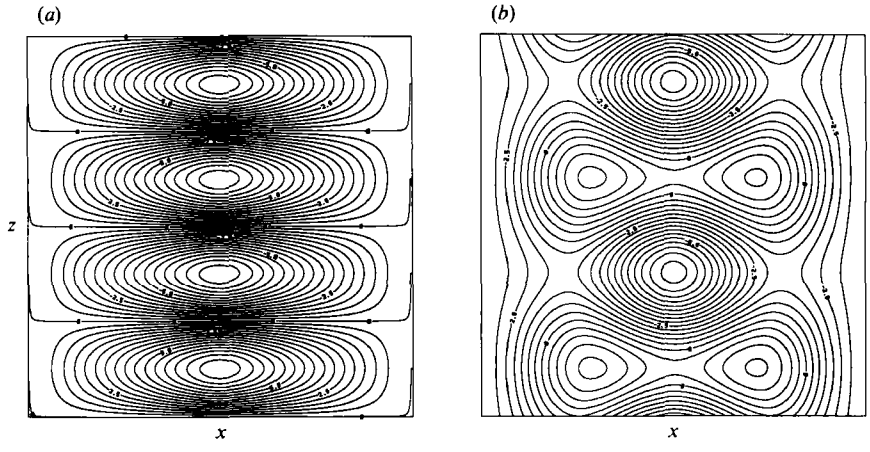

FIGURE 5. (a) The composite perturbation stream function, $\Psi(\lambda) + \Psi(\lambda^*)$, for the most unstable mode ($k = 0.5, m = 0.55$) when $Q = 1$. The horizontal range is one wavelength (two wavelengths of the steady flow) and the vertical range extends two wavelengths in z. Note the net horizontal flow either to the right or to the left at each value of z. The amplitudes oscillate with time. (b) $\Psi_s + 0.5(\Psi(\lambda) + \Psi(\lambda^*))$ for the same case showing time oscillating, net horizontal flow as a function of z.

number of fingers protruding into the reservoirs is half the number of fingers in the zone itself and the spacing is double.

As pointed out in the introduction, a value of Q near 1 for these long fingers means that the system is very stably stratified ($R_\rho \gg 1$) so the fluid moves slowly through the fingers and the effects of diffusion are important.

4. Discussion and conclusions

Our analysis concludes that the steady salt fingers derived by Howard & Veronis (1987) for $\tau \ll 1$ are unstable for all of the parameter range explored. If the stabilizing temperature difference has an effect on the density that is close to that of the

destabilizing salinity difference ($R_\rho \approx 1$), the most unstable mode grows without oscillation and has a vertical scale comparable to the buoyancy-layer thickness. For a very stably stratified fluid ($R_\rho \approx H/L \gg 1$) the most unstable mode has a somewhat smaller vertical scale but encompasses pairs of salt fingers, i.e. there is a kind of period doubling. In both situations the instability introduces a mean horizontal circulation that could cause the fingers to incline toward the horizontal. How effective the instability is in generating more horizontally oriented features is, of course, beyond the domain of linear theory.

We do not know how pertinent a stability analysis is to the salt-finger system. Very thin fingers form nearly instantaneously from an initial two-layer configuration. During this short period it is likely that the system is more appropriately described in terms of rapid transients. However, after this initial evolution the stability analysis for large values of Q should be pertinent and the system should become unstable to the direct modes shown in figure 3(*a*). Observations made during the Hele–Shaw cell (Taylor & Veronis 1986) experiments indicate that the instability equilibrates and leads to a corrugation of the fingers. As the system evolves, there is a continuing penetration of thicker fingers from the outer edges of the finger zone. These would gradually replace the corrugated fingers that are present but the newer fingers would themselves become unstable and corrugated. This sequence would be repeated as the thickness of the finger zone grows. Although the interaction of the fingers with the reservoirs above and below is not treated here, it is clearly going to affect the finger region itself, particularly if the salinity anomaly deposited in the reservoirs by the fingers is large and causes very active convection. That problem will require a treatment quite different from the one in this paper.

Our results may appear to differ from Stern's (1969) conclusion that the salt-finger system admits a collective instability. However, we have reported only the most unstable mode. There are many additional unstable modes, some with small k and therefore involving several fingers, but they have substantially smaller growth rates. If the (smaller scale) instability that we have derived here were to equilibrate at finite amplitude without changing the basic structure of the system significantly, one of the slower growing modes could become the dominant one.

Unfortunately, there are few laboratory studies with sufficient detail to reveal the existence of instabilities of the type derived here. The only evidence that we have of a disturbance with a vertical scale that of the buoyancy layer is from the Hele–Shaw cell experiments of Taylor & Veronis (1986) shown by Veronis (1987). For that experiment the disturbance resembling the one derived here appears to equilibrate at finite amplitude and the salt fingers look corrugated.

Most two-layer experiments with salt fingers (e.g. Turner 1973, plate 8.8) have large $\beta\Delta S$ so that the fingers that form appear irregularly wavy and the buoyant blobs that are deposited at the edges of the finger zone help to generate relatively active convective motions in the reservoirs. The convection interacts with the finger zone and may be so violent that the thickness of the finger zone becomes very small, not much bigger than a finger width. The larger-scale convective motions sweep away the buoyant blobs and the concomitant shear of the horizontal velocity can tilt the fingers toward the horizontal. When that happens, the basic configuration of the HV model is not realized and the stability analysis is not appropriate.

Even when $\beta\Delta S$ is large, as long as the overall density stratification is stable, the only way that the system can draw on the potential energy of the destabilizing salt is for diffusion to reduce the effect of the stable temperature field. Therefore, the horizontal scale of the basic disturbance must be of the order of the buoyancy layer

and the basic balance of the HV model will be important even though vertical variations may also contribute quantitatively. We have not tried to analyse the system with variation in the z-direction.

Eventually we would like to have an analysis that would be appropriate for oceanic observations. Several oceanographic expeditions have been undertaken to observe salt fingering in the ocean. The most ambitious was the CSALT expedition (Schmitt *et al.* 1987). The staircase structure showing layers with uniform T and S sandwiched between finger zones with uniform gradients of T and S is persistent east of the Caribbean, but local measurements did not reveal identifiable salt fingers (Kunze *et al.* 1987). The data distributed by the CSALT group are at 1 m intervals in the vertical, much too coarse to confirm the existence of individual salt fingers. Even so, the available measurements indicate a value of R_ρ around 1.6 over a 300 m depth interval. If long fingers exist, the direct instability derived above is pertinent. But if the 'fingers' are short, the fluid would traverse the finger zone before an instability could manifest itself and the stability analysis is not applicable. In that case, the system is probably best described in terms of an interaction of the reservoirs across a short transition region in which the HV model-balance releases the potential energy of the salt distribution as mentioned in the previous paragraph.

The work reported here should help to interpret results of a numerical study by Colin Shen of NRL. He has generated a regular array of salt fingers by suppressing perturbations and has also obtained a rather chaotic configuration from noisy initial conditions. It may be possible to relate the destabilizing elements to the modes derived here.

Support was provided by NSF Grants OCE84-10154, 86-00986 and 90-10662 and ONR Grants N00014-C-0873 NR 062-547 and N00014-89-j-1662. We are grateful to Will Morrell for writing some of the computer programs, to Edward Bolton for helpful discussions and to J. H. Lee for help with the contouring routine.

REFERENCES

HOWARD, L. N. & VERONIS, G. 1987 The salt finger zone. *J. Fluid Mech.* **183**, 1 (referred to herein as HV).

HUPPERT, H. E. & MANINS, P. C. 1973 Limiting conditions for salt fingering at an interface. *Deep-Sea Res.* **20**, 315.

KUNZE, E., WILLIAMS, A. J. & SCHMITT, R. W. 1987 Optical microstructure in the thermohaline staircase east of Barbados. *Deep-Sea Res.* **34**, 1697.

PRANDTL, L. 1952 *Essentials of Fluid Dynamics*. Hafner.

SCHMITT, R. W. 1979 The growth rate of supercritical salt fingers. *Deep-Sea Res.* **26A**, 23.

SCHMITT, R. W., PERKINS, H., BOYD, J. D. & STALCUP, M. C. 1987 C-SALT: an investigation of the thermohaline staircase in the western tropical North Atlantic. *Deep-Sea Res.* **34**, 1655.

STERN, M. E. 1960 The 'salt-fountain' and thermohaline convection. *Tellus* **12**, 172.

STERN, M. E. 1969 Collective instability of salt fingers. *J. Fluid Mech.* **35**, 209.

STERN, M. E. 1975 *Ocean Circulation Physics*, Chap. XI. Academic.

TAYLOR, J. & VERONIS, G. 1986 Experiments on salt fingers in a Hele Shaw cell. *Science* **23**, 39.

TURNER, J. S. 1973 *Buoyancy Effects in Fluids*. Cambridge University Press.

VERONIS, G. 1987 The role of the buoyancy layer in determining the structure of salt fingers. *J. Fluid Mech.* **180**, 327.